

Interferometric determination of the s- and d-wave scattering amplitudes in ^{87}Rb

Ch. Buggle, J. Leonard, W. von Kitzing, and J. T. M. Walraven

FOM Institute for Atomic and Molecular Physics, Kruislaan 407, 1098 SJ Amsterdam, The Netherlands and
Van der Waals-Zeeman Institute of the University of Amsterdam, Valckenierstraat 65/67, 1018 XE The Netherlands

(Dated: May 23, 2019)

We demonstrate an interference method for the determination of the low-energy elastic scattering amplitudes in a quantum gas. We collide two ultracold clouds at energies of up to 1.2 mK. Using computerized tomography to process the images of the scattering halos, we observe the s-d interference in the differential cross section. The accumulated phase method allows us to infer the s- and d-wave scattering amplitudes from the zero-energy limit up to the first Ramaker minimum, provided the Van der Waals C_6 coefficient is known. For ^{87}Rb we obtain $a = 102(6)a_0$ for the s-wave scattering length and 300(70) K for the location of the d-wave resonance.

PACS numbers: 34.50.-s, 32.80.Pj, 03.75.-b, 03.65.Sq

The scattering length a , the elastic scattering amplitude in the zero-energy limit, is the central parameter in the theoretical description of quantum gases [1, 2, 3]. It determines the kinetic properties of these gases as well as the bosonic mean field. Its sign is decisive for the collective stability of the Bose-Einstein condensed state. Near scattering resonances, pairing behavior [2] and three-body lifetime [3] can also be expressed in terms of a .

Over the past decade the crucial importance of the scattering length has stimulated important advances in collisional physics [4]. In all cases except hydrogen [5] the scattering length has to be determined experimentally as accurate *ab initio* calculations are not possible. An estimate of the modulus $|a|$ can be obtained relatively simply by measuring kinetic relaxation times [6]. In some cases the sign of a can be determined by such a method, provided p-wave or d-wave scattering can be neglected or accounted for theoretically [7]. Precision determinations are based on photo-association [8], vibrational Ramman [9] and Feshbach-resonance spectroscopy [10, 11], or a combination of those. They require close interplay between experiment and theory. This combination advanced the level of accuracy to the point that our knowledge of the interaction parameters in quantum gases rivals that for collisions of cold hydrogen atoms [11, 12].

In this Letter we present an interference method for the determination of the full s- and d-wave scattering amplitudes in a quantum gas. Colliding two ultracold atomic clouds we observe the scattering halo directly in the rest frame of the collisional center of mass. We accelerate the clouds up to energies at which the scattering pattern results from the interference between the s- and d-partial waves. Up to this point, our approach is similar to that of Ref. [13] in a jiggling atomic fountain. After applying a computerized tomography transformation [14] we obtain an angular distribution directly proportional to the differential cross section. This allows us to measure the asymptotic phase shifts $\chi(k)$ (with k the relative momentum) of the s-wave ($l=0$) and d-wave

($l=2$) scattering channels. By bosonic symmetry the odd partial waves are not excited. Using these $\chi(k)$ as boundary conditions, we integrate the radial Schrödinger equation inwards over the $C_6=r^6$ tail of the potential and compute the accumulated phase [15] of the wavefunction at radius $20a_0$ (with a_0 the Bohr radius). We fit all the experimental $\chi(k)$ to a single optimized accumulated phase from which we can infer all the low-energy scattering properties, by integrating again the same Schrödinger equation outwards. We demonstrate this method with ^{87}Rb atoms interacting through the ground-state triplet potential. We took data with both condensates and thermal clouds. Here we report on the condensates, as they allow to observe the largest range of scattering angles, $25^\circ < \theta < 90^\circ$. Up to 80% of the atoms are scattered without destroying the interference pattern. With our method, we obtain $a = +102(6)a_0$ for the scattering length. The d-wave resonance [16] is found at 300(70) K. For the location of the first Ramaker-Townsend minimum we obtain 2.1(2) mK. These results coincide within experimental error with the precision determinations [11, 12], and demonstrate the value of our approach as a stand-alone method for the determination of the low-energy elastic scattering properties of ultracold gases with minimal theoretical input.

In our experiments, we load about one billion ^{87}Rb atoms in the (fully stretched) $f=2; m_f=2$ hyperfine level of the electronic ground state from a magneto-optical trap (MOT) into a 10-ePritchard quadrupole trap (21–477 Hz) with an offset field of $B_0 = +0.9$ G. We pre-cool the sample to about 6 K using forced radio-frequency (RF) evaporation and split it in two. We apply a 1.22 G magnetic field rotating at 7 kHz orthogonally around the trap axis and ramp down the offset field in 0.4 s from the initial positive value of +0.9 G to a negative value B_0 in the range 9.2 G $< B_0 < 1.0$ G. This procedure developed previously [17] produces two time orbiting potential (TOP) traps loaded with thermal atoms and separated by as much as 3.6 mm for our largest negative offset field. Using forced RF-evaporation

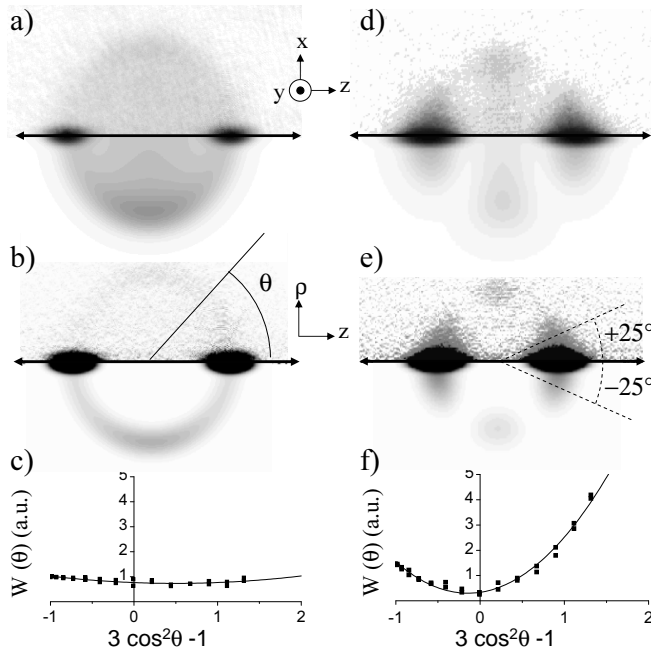


FIG. 1: a) Optical density of the scattering halo of two ^{87}Rb condensates for collision energy $E = k_B = 138(4)$ K, measured 2.4 ms after the collision (upper half: measured; lower half: calculated [21]); b) radial density distribution obtained after tomography transformation of image a (upper half: measured; lower half: calculated [21]); c) the dots show the angular scattering distribution $W(\theta)$ obtained after binning plot b, the line is the best parabolic fit. d,e,f) As in plots a,b,c, but measured 0.5 ms after a collision at 1230(40) K. The field of view of the images is $1 \times 1 \text{ mm}^2$.

we cool the clouds until we reach Bose-Einstein condensation with about 10^5 atoms in each cloud and a condensate fraction of 50–75%.

We then switch off the TOP fields and ramp the offset field back to positive values of B_0 , thus accelerating the clouds until they collide with opposite horizontal momenta at the location of the trap center [18]. Conveniently, the collision energy depends only on the modulus of the negative offset field, $E = \frac{1}{2} B_0 j = \frac{1}{2} k^2 m$ (with m the mass of ^{87}Rb). The collision energies range from 138 K to 123 mK with an overall uncertainty of 3% (RMS) [19]. Approximately 0.5 ms before the collision we switch off the trap. A few ms after the collision, we observe the scattering halo using absorption imaging. Fig. 1a (upper part) shows the result for a collision energy of $E = k_B = 138(4)$ K after averaging over 20 pictures. We recognize the s-wave-dominated halo of fully entangled pairs previously studied at MIT [20]. In Fig. 1d (upper part), taken at $E = k_B = 123(4)$ mK the halo is entirely different, showing a d-wave-dominated pattern. The lower halves of Fig. 1a and Fig. 1d show the theoretical column densities $n_2(x; z) = \int n(x; y; z) dy$, where $n(x; y; z)$ is the calculated [21] density of the halo.

The data analysis proceeds in five steps. As the atoms are scattered by a central field, the scattering pattern must be axially symmetric around the (horizontal) scattering axis (z -axis). As pointed out by the Weizmann group [22], this allows a computerized tomography transformation [14] to reconstruct the radial density distribution of the halo in cylindrical coordinates,

$$n(x; z) = \frac{1}{4} \int_{-1}^{Z_1} n_2(x; z) J_0(x) j_x j_d x : \quad (1)$$

Here $x = \sqrt{x^2 + y^2}$, $n_2(x; z)$ is the 1D Fourier transform along the x -direction of the optical density with respect to z , and $J_0(x)$ is the zero-order Bessel function. The transformed plots corresponding to the images of Fig. 1a,d are shown as Fig. 1b,e respectively.

In the second step of the analysis, we bin the tomography pictures in 40 discrete angular sectors to obtain the angular scattering distribution $W(\theta)$. For gas clouds much smaller than the diameter of the halo, $W(\theta)$ is directly proportional to the differential cross section

$(\theta) = 2 \int f(\theta) + f(\theta) j_d$. Here, the Bose-symmetrized scattering amplitude is given by a summation over the even partial waves, $f(\theta) + f(-\theta) = (2=k) \sum_{l=even} (2l+1) e^{i l} P_l(\cos \theta) \sin \theta$. Integrating (θ) over all distinguishable scattering angles, the interference cross terms between the various partial waves cancel to yield the well-known result for the total elastic cross section:

$$= \int_0^{\pi} (\theta) \sin \theta = (8 \pi^2 k) \sum_{l=even} (2l+1) \sin^2 \theta.$$

However, in the differential cross section the interference is prominent. Given the small collision energy in our experiments, only the s- and d-wave scattering amplitudes contribute, $f_s(\theta) + f_s(-\theta) = (2=k) e^{i 0} \sin \theta$ and $f_d(\theta) + f_d(-\theta) = (2=k) (5=2) e^{i 2} \sqrt{3} \cos^2 \theta \sin \theta$. Therefore the differential cross section is given by

$$(\theta) = \frac{8}{k^2} \sin^2 \theta + 5 \cos(\theta - \pi/2) u + \frac{25}{4} u^2 ; \quad (2)$$

where $u = (\sin \theta - \sin \theta_0) / \sqrt{3 \cos^2 \theta - 1}$.

Turning to the third step of our analysis, we plot the measured angular distribution $W(\theta)$, for each collision energy, as a function of $3\cos^2 \theta - 1$ as suggested by Eq. (2). The results for Fig. 1a and Fig. 1d are shown as the solid dots in Fig. 1c and Fig. 1f, respectively. Since (θ) is a parabola in the variable $3\cos^2 \theta - 1$, with coefficients depending on $\theta_0(k)$ and $\theta_2(k)$, we fit (θ) to a parabola. The result of the fit is a pair $f_0(k), f_2(k)$ of asymptotic phase shifts (defined modulo π) corresponding to the two partial waves involved (except for the marginal case $\theta_0 = \theta_2$, where the expression in the square brackets in Eq. (2) becomes phase-shift independent). The absolute value of $W(\theta)$ depends on quantities that are hard to measure accurately (like the atom number) so we leave it out of consideration. We rather emphasize that the measurement of the phase shifts is a complete determination of the (complex) s- and d-wave

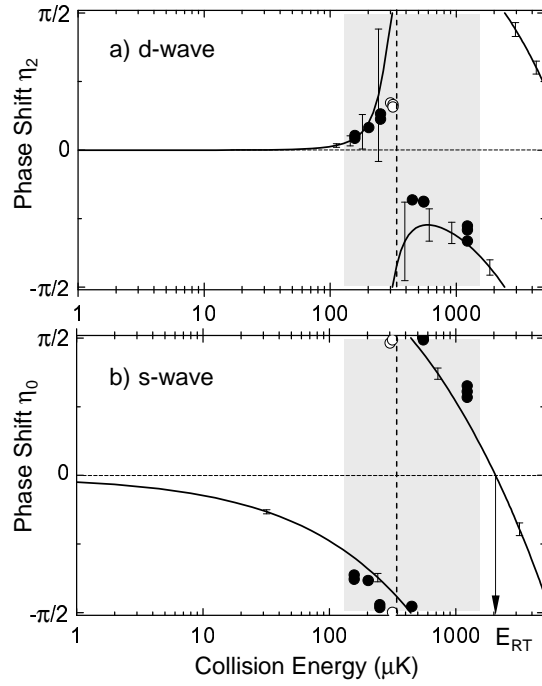


FIG. 2: a) d-wave and b) s-wave phase shifts versus collision energy in m K. The circles are the results of the parabolic t of $W(\mathbf{k})$ for individual images. The full lines are calculated from the accumulated phase η_{opt} optimized from all the data points (the vertical dotted line indicates the condition $\eta_0 = \eta_2$). s-d interference is only observed in the gray areas. The first s-wave Ram sauer-Townsend minimum is found at $E_{\text{RT}} = 2.1(2)$ m K.

scattering amplitudes at a given energy. However, there is a caveat. Since Eq. (2) is unchanged under reversal of the sign of both asymptotic phase shifts, the result of the t is not unique: only one pair $f_0(\mathbf{k})$; $f_2(\mathbf{k})g$ or $f_0(\mathbf{k})$; $f_2(\mathbf{k})g$ can be physically correct.

In the fourth step we eliminate this ambiguity. We calculate the accumulated phase $\eta(r)$ of the radial wavefunction at radius $r_{\text{in}} = 20 a_0$ by integrating the radial Schrödinger equation, for both $l=0$ and $l=2$, over the $C_6=r^6$ tail of the potential, starting from experimentally determined asymptotic values $\eta_0(\mathbf{k})$ and $\eta_2(\mathbf{k})$. The value $r_{\text{in}} = 20 a_0$ is small enough [23] for $\eta(r_{\text{in}})$ to be highly insensitive to small variations in E or l [15] and large enough that the $C_6=r^6$ part of the interaction potential is dominant over the full range of integration. To determine the correct signs for $f_0(\mathbf{k})$; $f_2(\mathbf{k})g$, we simply compare the accumulated phase $\eta(r_{\text{in}})$ obtained for $\eta_0(\mathbf{k})$ and for $\eta_2(\mathbf{k})$. We then switch the signs of $\eta_0(\mathbf{k})$ and $\eta_2(\mathbf{k})$, and again calculate the accumulated phases for both. We find that in almost all cases, the accumulated phases corresponding to one choice of signs for $\eta_0(\mathbf{k})$ and $\eta_2(\mathbf{k})$ are in much closer agreement. If we are to believe the validity of the accumulated phase approximation, we must conclude that the correct sign for a

pair $f_0(\mathbf{k})$; $f_2(\mathbf{k})g$ is the one for which the accumulated phases agree best. We next calculate the standard deviation SD in the preferred values for (r_{in}) . In only three cases (at the same collision energy), the accumulated phases calculated using different sign choices for $f_0(\mathbf{k})$, $f_2(\mathbf{k})g$ differed by less than 1° . In the following we omit these energies, and are left with $N = 11$ pairs $f_0(\mathbf{k}_i)$, $f_2(\mathbf{k}_i)g$, $i = 1; N$.

In the final step of our analysis, we fit the whole set of $2N$ experimental phase shifts $\eta_1^{\text{exp}}(\mathbf{k}_i)$, $i = 0; 2$ to obtain a single optimized value η_{opt} for the accumulated phase at $20 a_0$. The optimization is done such that after integrating the Schrödinger equation outward, the standard deviation $\text{SD} = (2N - 1) \sqrt{\frac{1}{N} \sum_{i=1}^N (\eta_1^{\text{exp}}(\mathbf{k}_i) - \eta_1^{\text{opt}}(\mathbf{k}_i))^2}$ of the phase shifts $\eta_1^{\text{opt}}(\mathbf{k})$, corresponding to η_{opt} , is minimized. Interestingly, the d-wave scattering resonance [16] results in a sudden variation of η_2^{exp} with the collision energy in the vicinity of that resonance (see Fig. 2a). This imposes a stringent condition on the optimization of η_{opt} . Consequently, the uncertainty in η_{opt} is rather small and is estimated to be ± 0.025 .

Once the optimized accumulated phase η_{opt} has been established one can integrate the Schrödinger equation outwards to compute $\eta_1(\mathbf{k})$ for any desired (low) value of \mathbf{k} and l . Fig. 2 shows the resulting phase shifts $\eta_0(\mathbf{k})$ and $\eta_2(\mathbf{k})$ for collision energies up to 5 m K [24], with error bars corresponding to the ± 0.025 uncertainty in η_{opt} . The solid dots represent the $\eta_1^{\text{exp}}(\mathbf{k}_i)$ obtained from the t of individual images. The three open circles correspond to the measurements for which the sign of the phase shifts could not be established.

Knowing the phase shifts, we can infer all the low-energy scattering properties. Our results for the elastic scattering cross section are shown in Fig. 3. The first Ram sauer-Townsend minimum in the s-wave cross section [25] is found at collision energy $E_{\text{RT}} = K_B = 2.1(2)$ m K. The (asymmetric) d-wave resonance emerges pronouncedly at $300(70)$ K with an approximate width of 150 K (FWHM). Most importantly, the scattering length follows from the $k \rightarrow 0$ limiting behavior, $a(\mathbf{k} \rightarrow 0) = -ka$. We find $a = +102(6) a_0$, whereas the state-of-the-art value is $a = 98.99(2) a_0$ [12].

Comparison with the precision determination [11, 12] shows that our method readily yields fairly accurate results, relying only on input of the C_6 coefficient. We used the value $C_6 = 4.698(4) \times 10^3$ a.u. [12]. However, one does not need to know C_6 to this accuracy. Increasing C_6 by 10% results in a 1% change of the scattering length. Clearly, the error accumulated when determining η_{opt} by integrating the Schrödinger equation inward with a wrong C_6 largely cancels when integrating back outward again.

This method can also be applied to other bosonic or fermionic atomic species, provided the gases can be cooled and accelerated in such a way that the lowest-

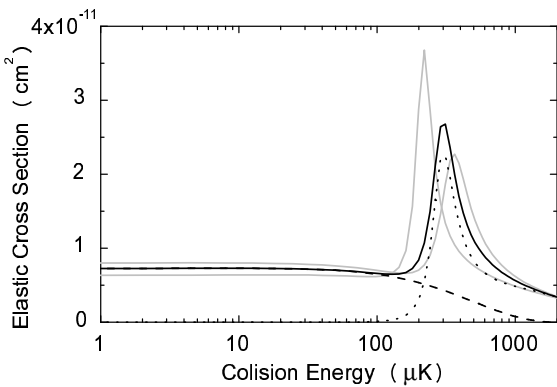


FIG. 3: s-wave (dashed line), d-wave (dotted line) and total (full black line) elastic cross sections (in cm^2) versus collision energy (in K), computed from the optimized accumulated phase ϕ_{opt} as determined in this work. The gray lines are the total elastic cross sections, obtained from $\phi_{\text{opt}} = 0.025$.

order partial-wave interference can be observed with good energy resolution. We speculate that the accuracy of the method can be strongly improved by turning to smaller optical-density clouds and fluorescence detection. It will enable higher collision energies and observation of higher-order partial-wave interference. The use of more dilute clouds and longer expansion times will also eliminate multiple-scattering effects and finite-size convolution broadening of the interference pattern. Finally it will enable precision measurements of the scattered fraction, which in the case of ^{87}Rb will allow us to pinpoint the location of the d-wave resonance to an accuracy of 10 K or better. In combination with state-of-the-art theory such improvements are likely turn our approach into a true precision method.

Similar experiments were reported during the final stage of completion of this Letter [26].

The authors acknowledge valuable discussions with Servaas Kokkelmans, Dima Petrov, Gora Shlyapnikov, Steve Gensemer and Boudeijn Verhaar. This work is part of the research programme of the Stichting voor Fundamenteel Onderzoek der Materie (FOM), which is financially supported by the Nederlandse organisatie voor Wetenschappelijk Onderzoek (NWO). JL acknowledges support from a Marie Curie Intra-European Fellowship (MEXT-CT-2003-501578).

[1] See e.g. L.Pitaevskii and S.Stringari, *Bose-Einstein condensation*, Clarendon Press, Oxford 2003; C.J.Pethick and H.Smith, *Bose-Einstein condensation in dilute gases*, Cambridge University Press, Cambridge 2002.

[2] D.S.Petrov, C.Salomon and G.V.Shlyapnikov, cond-mat/0309010.

[3] P.O.Fedichev, M.W.Reynolds and G.V.Shlyapnikov, Phys.Rev.Lett. 77, 2921 (1996).

[4] J.W.Bauer, V.S.Bagnato, S.Zilio, and P.S.Julienne, Rev.Mod.Phys. 71, 1 (1999).

[5] D.G.Friend and R.D.Etters, J.Low Temp.Phys. 39, 409 (1980); Y.H.Uang and W.C.Stwalley, J.de Phys. 41, C7-33 (1980).

[6] C.R.Morroe et al., Phys.Rev.Lett. 70, 414 (1993); S.D.Gensemer et al., Phys.Rev.Lett., 87, 173201 (2001).

[7] G.Ferrari et al., Phys.Rev.Lett. 89, 53202 (2002); P.Schmid et al., Phys.Rev.Lett. 91, 193201 (2003).

[8] D.Heinzen, in: *Proceedings of the international School of Physics - Enrico Fermi*, M.Inguscio, S.Stringari and C.William (Eds.), IOS Press, Amsterdam 1999.

[9] C.Samuelis et al., Phys.Rev.A 63, 12710 (2001).

[10] C.Chin, V.Vuletic, A.J.Kerman, and S.C.Chu, Phys.Rev.Lett. 85, 2717 (2000); P.J.Leo, C.J.Williams, and P.S.Julienne, Phys.Rev.Lett. 85, 2721 (2002).

[11] A.Marte et al., Phys.Rev.Lett. 89, 283202 (2002).

[12] E.G.M.van Kempen, S.J.J.M.F.Kokkelmans, D.J.Heinzen, and B.J.Verhaar, Phys.Rev.Lett. 88, 93201 (2002); B.J.Verhaar and S.J.J.M.F.Kokkelmans, private communications.

[13] R.Legere and K.Gibble, Phys.Rev.Lett. 81, 5780 (1998).

[14] M.Born and E.Wolf, *Principles of Optics*, 7th (expanded) Edition, Cambridge University Press, Cambridge 1999.

[15] B.Verhaar, K.Gibble, and S.C.Chu, Phys.Rev.A 48, R3429 (1993); G.F.Gribakin and V.V.Flambaum, Phys.Rev.A 48, 546 (1993).

[16] H.M.J.M.Boesten, C.C.Tsai, J.R.Gardner, D.J.Heinzen, B.J.Verhaar, Phys.Rev.A 55, 636 (1997).

[17] T.G.Tiedke et al., J.Opt.B 5, S119 (2003); see also N.R.Thomas, A.C.Wilson, and C.J.Foot, Phys.Rev.A 65, 063406 (2002).

[18] To avoid excitation of shape oscillations, the offset ramp is done in such a way that the radial component frequency at the location of the clouds remains approximately constant during the acceleration.

[19] B_0 is calibrated using RF-depletion of condensates at positive B_0 . We checked that the collision energy \mathcal{E}_{B_0} agrees within 2% with a calibration based on direct measurement of the relative velocity. The magnification of our imaging system is calibrated against the gravity acceleration of $m_F = 0$ clouds.

[20] A.P.Chikkatur et al., Phys.Rev.Lett., 85, 483 (2000); J.M.Vogels, K.Xu, and W.Ketterle, Phys.Rev.Lett. 89, 20401 (2002).

[21] Based on the phase shifts reported in this Letter.

[22] R.Ozeri, J.Steinbauer, N.Katz, and N.Davidson, Phys.Rev.Lett., 88, 220401, (2002).

[23] We checked that, within the range $15a_0 < r < 25a_0$, the exact choice of the inner radius of the integration interval is of no influence for the results presented in this Letter.

[24] The g-wave ($l = 4$) phase shift can also be computed from the same ϕ_{opt} , but the error made by assuming a constant accumulated phase increases like $l(l+1)$, and the resulting g-wave would be accordingly less accurate.

[25] Ramsauer-Townsend minima are observed around collision energies where a phase shift crosses zero (see Fig.2).

[26] N.R.Thomas, N.Kjørgaard, P.S.Julienne, and A.C.Wilson, cond-mat/0405544.

[1] See e.g. L.Pitaevskii and S.Stringari, *Bose-Einstein condensation*, Clarendon Press, Oxford 2003; C.J.Pethick and H.Smith, *Bose-Einstein condensation in dilute gases*, Cambridge University Press, Cambridge 2002.

[2] D.S.Petrov, C.Salomon and G.V.Shlyapnikov, cond-mat/0309010.

[3] P.O.Fedichev, M.W.Reynolds and G.V.Shlyapnikov,